A Real-Time *QRS* Detection Algorithm

JIAPU PAN AND WILLIS J. TOMPKINS, SENIOR MEMBER, IEEE

***Abstract*—We have developed a real-time algorithm for detection of the *QRS* complexes of ECG signals. It reliably recognizes *QRS* complexes based upon digital analyses of slope, amplitude, and width. A special digital bandpass filter reduces false detections caused by the various types of interference present in ECG signals. This filtering permits use of low thresholds, thereby increasing detection sensitivity. The algorithm automatically adjusts thresholds and parameters periodically to adapt to such ECG changes as *QRS* morphology and heart rate. For the standard 24 h MIT/BIH arrhythmia database, this algorithm correctly detects 99.3 percent of the *QRS* complexes.**

INTRODUCTION

THERE are many uses for a reliable *QRS* recognition algorithm. Computer interpretation of the 12-lead ECG is a popular technique. Coronary care units now use arrhythmia monitors extensively. Widely used Holter tape recording requires a Holter scanning device that includes a *QRS* detector to analyze the tapes much faster than real time. Currently under development are arrhythmia monitors for ambulatory patients which analyze the ECG in real time [1]–[3]. When an arrhythmia appears, such a monitor can be programmed to immediately store an interval of the abnormal ECG for subsequent transmission to a central station where a physician can interpret it. Such a device requires a very accurate *QRS* recognition capability. False detection results in unnecessary transmission of data to the central station or requires an excessively large memory to store any ECG segments that are unnecessarily captured. Thus, an accurate *QRS* detector is an important part of many ECG instruments.

QRS detection is difficult, not only because of the physiological variability of the *QRS* complexes, but also because of the various types of noise that can be present in the ECG signal. Noise sources include muscle noise, artifacts due to electrode motion, power-line interference, baseline wander, and *T* waves with high-frequency characteristics similar to *QRS* complexes. In our approach, digital filters reduce the influence of these noise sources, and thereby improve the signal-to-noise ratio. Of the many *QRS* detectors proposed in the literature, few give serious enough attention to noise reduction.

Software *QRS* detectors typically include one or more of three different types of processing steps: linear digital filtering, nonlinear transformation, and decision rule algorithms [4]. We use all three types. Linear processes include a bandpass filter, a derivative, and a moving window integrator. The nonlinear transformation that we use is signal amplitude squaring. Adaptive thresholds and *T*-wave discrimination techniques provide part of the decision rule algorithm.

The slope of the *R* wave is a popular signal feature used to locate the *QRS* complex in many *QRS* detectors [5]. An analog circuit or a real-time derivative algorithm that provides slope information is straightforward to implement. However, by its very nature, a derivative amplifies the undesirable higher frequency noise components. Also, many abnormal *QRS* complexes with large amplitudes and long durations are missed in a purely derivative approach because of their relatively low *R*-wave slopes. Thus, *R*-wave slope alone is insufficient for proper *QRS* detection. To achieve reliable performance, we must extract other parameters from the signal such as amplitude, width, and *QRS* energy [6], [7].

It is very important to evaluate a *QRS* detector algorithm using a standard arrhythmia database. There are now two such databases available: MIT/BIH [8] and AHA (American Heart Association) [9]. The performance of an algorithm on a database is not the ultimate answer as to its utility in a clinical environment, but it provides a standardized means of comparing the basic performance of one algorithm to another.

ALGORITHM OVERVIEW

xd

We implemented the *QRS* detection algorithm in assembly language. It operates on either a Z80 (Zilog) or an NSC800 (National Semiconductor) microprocessor. All the processing is done with integer arithmetic so that the algorithm can operate in real time without requiring excessive computing power. The database provides two simultaneous ECG channels. We attempted two-channel analysis, but abandoned this approach. Due to the way that the electrode positions are orthogonally placed in Holter recording, a high-quality signal on one channel normally implies a low-amplitude ECG with a poor signal-to-noise ratio on the second channel. The only way that two-channel algorithms will yield improved performance for most patients is by adopting a new way of electrode placement that will provide usable signals in both channels.

Fig. 1 shows signals at various steps in digital signal processing. First, in order to attenuate noise, the signal passes through a digital bandpass filter composed of cascaded high-pass and low-pass filters. Fig. 1(b) shows the output of this filter. The next process after filtering is differentiation [see Fig. 1(c)], followed by squaring [see Fig. 1(d)], and then moving window integration [see Fig. 1(e)]. Information about the slope of the *QRS* is obtained in the derivative stage. The squaring process intensifies the slope of the frequency response curve of the derivative and helps restrict false positives caused by *T* waves with

Manuscript received July 27, 1984; revised October 24, 1984. This work was supported in part by the National Institutes of Health under Grant HL00765.

J. Pan is with the Department of Biophysics, Shanghai Second Medical College, Shanghai, People's Republic of China.

W. J. Tompkins is with the Department of Electrical and Computer Engineering, University of Wisconsin, Madison, WI 53706.

0018-9294/85/0300-0230$01.00 © 1985 IEEE

pasos que hace la parte de fintrado lineal

pasos no lineales usados

pasos que toma el algoritmo de desición

por que solo derivar no es suficiente para detectar complejo QRS

por qué no usaron los 2 canales de señal ecg.

tipos de ruido en una señal ecg

pasos tipicos de procesamiento de señal ecg

atenuación de ruido con un pasabandas

lo que hace la etapa de derivada y el aplicar el cuadrado a la señal

paso a paso del proceso con imagenes iterativas que ilustran todo lo que va sucediendo

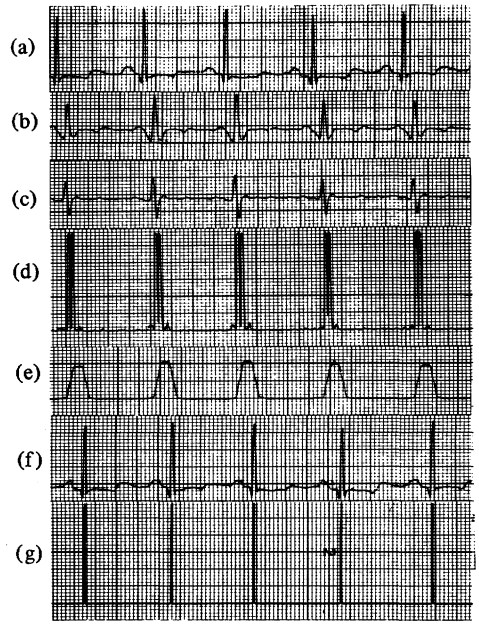

Fig. 1. *QRS* detection algorithm processing steps for a normal ECG from the MIT/BIH database. (a) Original signal. (b) Output of bandpass filter. (c) Output of differentiator. (d) Output of squaring process. (e) Results of moving-window integration. (f) Original ECG signal delayed by the total processing time. (g) Output pulse stream.

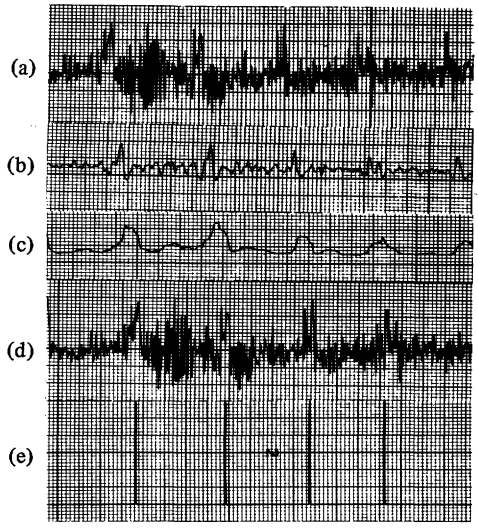

Fig. 2. *QRS* detection algorithm processing steps for a noise-contaminated ECG from the MIT/BIH database. (a) Original signal. (b) Output of bandpass filter. (c) Results of moving-window integration. (d) Original ECG signal delayed by the total processing time. (e) Output pulse stream.

lo que hace la ventana integradora que se va moviendo

higher than usual spectral energies. The moving window integrator produces a signal that includes information about both the slope and the width of the *QRS* complex. Fig. 1(f) is the same as the original ECG in Fig. 1(a) except delayed by the total processing time of the detection algorithm. Fig. 1(g) shows the final output stream of pulses marking the locations of the *QRS* complexes after application of the adaptive thresholds.

Fig. 2 illustrates a set of signals similar to those in Fig. 1 for a noise-contaminated ECG in the database. The algorithm is able to correctly detect *QRS* complexes in the presence of the severe noise typical of the ambulatory ECG environment. We based all judgments of correctness upon the annotations in the database. Each annotation on the location and morphology of a beat was determined by arbitration between two cardiologists who had to be in agreement on all beats in order for an ECG data segment to be placed in the database.

The algorithm is divided into three processes: learning phase 1, learning phase 2, and detection. Learning phase 1 requires about 2 s to initialize detection thresholds based upon signal and noise peaks detected during the learning process. Learning phase 2 requires two heartbeats to initialize *RR*-interval average and *RR*-interval limit values. The subsequent detection phase does the recognition process and produces a pulse for each *QRS* complex. The thresholds and other parameters of the algorithm are adjusted periodically to adapt to changing characteristics of the signal.

usar 2 tipos de umbrales para detectar QRS aumenta la confiabilidad.

We use two sets of thresholds to detect *QRS* complexes. One set thresholds the filtered ECG, and the other thresholds the signal produced by moving window integration. By using thresholds on both signals, we improve the reliability of detection compared to using one waveform alone. Preprocessing the ECG with this digital bandpass filter improves the signal-to-noise ratio and permits the use of lower thresholds than would be possible on the unfiltered ECG. This increases the overall detection sensitivity. The detection thresholds float over the noise that is sensed by the algorithm. This approach reduces the number of false positives caused by types of noise that mimic the characteristics of the *QRS* complex.

utilidad de la tecnica de 2 umbrales

The algorithm uses a dual-threshold technique to find missed beats, and thereby reduce false negatives. There are two separate threshold levels in each of the two sets of thresholds. One level is half of the other. The thresholds continuously adapt to the characteristics of the signal since they are based upon the most-recent signal and noise peaks that are detected in the ongoing processed signals. If the program does not find a *QRS* complex in the time interval corresponding to 166 percent of the current average *RR* interval, the maximal peak detected in that time interval that lies between these two thresholds is considered to be a possible *QRS* complex, and the lower of the two thresholds is applied. In this way, we avoid requiring a long memory buffer for storing the past history of the ECG, and thus require minimal computing time to accomplish the search-back procedure to look for a missing *QRS* complex.

sobre los umbrales y la adaptación de sus niveles

casos en los que falla la aproximación de usar 2 umbrales, y como lo solucionan

Unfortunately, the dual-threshold technique is only useful if the heart rate is regular. In abnormalities such as bigeminy or trigeminy, we cannot find the missed beat by searching back through the same time interval as for regular heart rates. For the case of irregular heart rates, both thresholds are reduced by half in order to increase the sensitivity of detection and to avoid missing valid beats.

como usan la fisiologia y los timing del cuerpo a favor de hacer el algoritmo más robusto.

Once a valid *QRS* complex is recognized, there is a 200 ms refractory period before the next one can be detected since *QRS* complexes cannot occur more closely than this physiologically. This refractory period eliminates the possiblity of a false detection such as multiple triggering on the same *QRS* complex during this time interval. When a *QRS* detection

como usan la fisiologia y los timing del cuerpo a favor de hacer el algoritmo más robusto.

occurs following the end of the refractory period but within 360 ms of the previous complex, we must determine if it is a valid *QRS* complex or a *T* wave. In this case, we judge the waveform with the largest slope to be the *QRS* complex.

algoritmo en fun. del tiempo y sus adaptaciones

To be reliable, a *QRS* detection algorithm must adapt each of its parameters with time so as to be able to operate properly for ECG's of different patients as well as for ECG morphology changes in a single patient. In our algorithm, each threshold automatically adapts periodically based upon peak values of signal and noise. When a *QRS* must be found using second (lower) thresholds, threshold readjustment occurs twice as fast as usual. In the dual-threshold technique, the *RR*-interval average must be updated for each heartbeat.

sobre el intervalo RR y su adaptación.

Two separate measurements of the average *RR* interval are maintained. One *RR*-interval average is the mean of all of the most recent eight *RR* intervals. A second *RR*-interval average is the mean of the most recent eight beats that fell within the range of 92–116 percent of the current *RR*-interval average. Without this first average, this approach would be suitable only for a slowly changing and regular heart rate. When the heart rate suddenly changes, the first *RR*-interval average substitutes for the second one. The algorithm adapts rapidly to a changing signal. It can even adapt rapidly when switching from one patient's ECG to another without requiring special learning phases.

Methods

An analog filter bandlimits the ECG signal at 50 Hz. An analog-to-digital converter (ADC) samples the ECG at a rate of 200 samples/s. The resulting digital signal passes successively through a sequence of processing steps that includes three linear digital filters implemented in software. First is an integer-coefficient bandpass filter composed of cascaded low-pass and high-pass filters. Its function is noise rejection. Next is a filter that approximates a derivative. After an amplitude squaring process, the signal passes through a moving-window integrator. Adaptive thresholds then discriminate the locations of the *QRS* complexes.

Bandpass Filter

The bandpass filter reduces the influence of muscle noise, 60 Hz interference, baseline wander, and *T*-wave interference. The desirable passband to maximize the *QRS* energy is approximately 5–15 Hz [10], [11]. Our filter is a fast, real-time recursive filter in which poles are located to cancel zeros on the unit circle of the *z* plane [12]. This approach results in a filter design with integer coefficients. Since only integer arithmetic is necessary, a real-time filter can be implemented with a simple microprocessor and still have available computing power left to do the *QRS* recognition task.

This class of filters having poles and zeros only on the unit circle permits limited passband design flexibility. For our chosen sample rate, we could not design a bandpass filter directly for the desired passband of 5–15 Hz using this specialized design technique. Therefore, we cascaded the low-pass and high-pass filters described below to achieve a 3 dB passband from about 5–12 Hz, reasonably close to the design goal. Fig. 3 shows the overall frequency response.

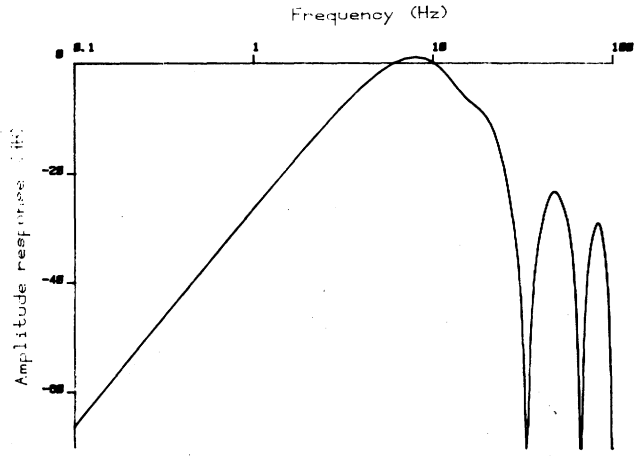

Fig. 3. Amplitude response of the digital bandpass filter. Passband (3 dB) is 5–11 Hz.

Low-Pass Filter

The transfer function of the second-order low-pass filter is

$$H(z) = \frac{(1 - z^{-6})^2}{(1 - z^{-1})^2}. \tag{1}$$

The amplitude response is

$$|H(wT)| = \frac{\sin^2(3\omega T)}{\sin^2(\omega T/2)} \tag{2}$$

where T is the sampling period. The difference equation of the filter is

$$y(nT) = 2y(nT - T) - y(nT - 2T) + x(nT) - 2x(nT - 6T) + x(nT - 12T) \tag{3}$$

where the cutoff frequency is about 11 Hz and the gain is 36. The filter processing delay is six samples.

High-Pass Filter

The design of the high-pass filter is based on subtracting the output of a first-order low-pass filter from an all-pass filter (i.e., the samples in the original signal). The transfer function for such a high-pass filter is

$$H(z) = \frac{(-1 + 32z^{-16} + z^{-32})}{(1 + z^{-1})}. \tag{4}$$

The amplitude response is

$$|H(wT)| = \frac{[256 + \sin^2(16\omega T)]^{1/2}}{\cos(wT/2)}. \tag{5}$$

The difference equation is

$$y(nT) = 32x(nT - 16T) - [y(nT - T) + x(nT) - x(nT - 32T)]. \tag{6}$$

The low cutoff frequency of this filter is about 5 Hz, the gain is 32, and the delay is 16 samples.

Derivative

After filtering, the signal is differentiated to provide the *QRS*-complex slope information. We use a five-point derivative with

the transfer function

$$H(z) = (1/8T)(-z^{-2} - 2z^{-1} + 2z^{1} + z^{2}). \quad (7)$$

The amplitude response is

$$|H(wT)| = (1/4T)[\sin(2\omega T) + 2\sin(\omega T)]. \quad (8)$$

The difference equation is [7]

$$y(nT) = (1/8T)[-x(nT - 2T) - 2x(nT - T) + 2x(nT + T) + x(nT + 2T)]. \quad (9)$$

Fig. 4 shows that the frequency response of this derivative is nearly linear between dc and 30 Hz (i.e., it approximates an ideal derivative over this range). Its delay is two samples.

Squaring Function

After differentiation, the signal is squared point by point. The equation of this operation is

$$y(nT) = [x(nT)]^2. \quad (10)$$

This makes all data points positive and does nonlinear amplification of the output of the derivative emphasizing the higher frequencies (i.e., predominantly the ECG frequencies).

Moving-Window Integration

The purpose of moving-window integration is to obtain waveform feature information in addition to the slope of the *R* wave. It is calculated from

$$y(nT) = (1/N)[x(nT - (N - 1)T) + x(nT - (N - 2)T) + \cdots + x(nT)] \quad (11)$$

where N is the number of samples in the width of the integration window.

Fig. 5 shows the relationship between the moving-window integration waveform and the *QRS* complex. The number of samples N in the moving window is important. Generally, the width of the window should be approximately the same as the widest possible *QRS* complex. If the window is too wide, the integration waveform will merge the *QRS* and *T* complexes together. If it is too narrow, some *QRS* complexes will produce several peaks in the integration waveform. These can cause difficulty in subsequent *QRS* detection processes. The width of the window is determined empirically. For our sample rate of 200 samples/s, the window is 30 samples wide (150 ms).

Fiducial Mark

The *QRS* complex corresponds to the rising edge of the integration waveform. The time duration of the rising edge is equal to the width of the *QRS* complex. A fiducial mark for the temporal location of the *QRS* complex can be determined from this rising edge according to the desired waveform feature to be marked such as the maximal slope or the peak of the *R* wave.

Adjusting the Thresholds

The thresholds are automatically adjusted to float over the noise. Low thresholds are possible because of the improvement of the signal-to-noise ratio by the bandpass filter.

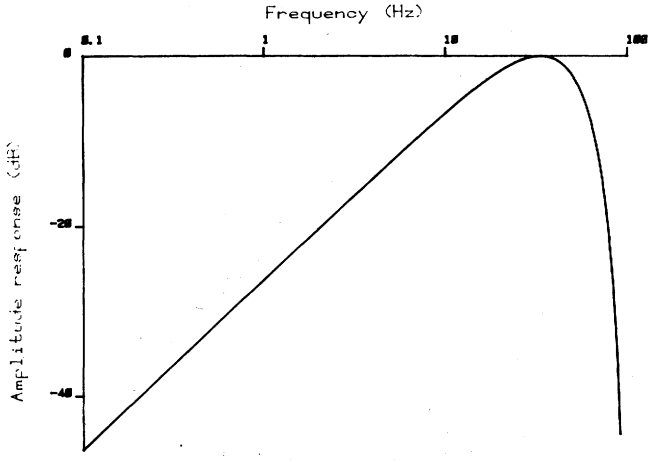

Fig. 4. Amplitude response of the digital derivative filter.

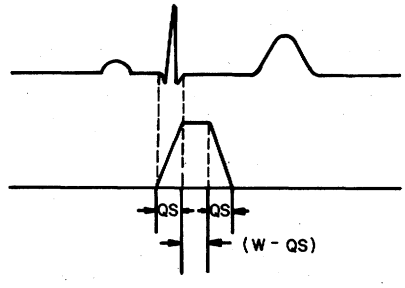

Fig. 5. The relationship of a *QRS* complex to the moving integration waveform. (a) ECG signal. (b) Output of moving-window integrator. *QS*: *QRS* width. *W*: width of the integrator window.

The higher of the two thresholds in each of the two sets is used for the first analysis of the signal. The lower threshold is used if no *QRS* is detected in a certain time interval so that a search-back technique is necessary to look back in time for the *QRS* complex. The set of thresholds initially applied to the integration waveform is computed from

$$\text{SPKI} = 0.125\ \text{PEAKI} + 0.875\ \text{SPKI} \quad \text{(if PEAKI is the signal peak)} \quad (12)$$

$$\text{NPKI} = 0.125\ \text{PEAKI} + 0.875\ \text{NPKI} \quad \text{(if PEAKI is the noise peak)} \quad (13)$$

$$\text{THRESHOLD I1} = \text{NPKI} + 0.25\ (\text{SPKI} - \text{NPKI}) \quad (14)$$

$$\text{THRESHOLD I2} = 0.5\ \text{THRESHOLD I1} \quad (15)$$

where all the variables refer to the integration waveform:

PEAKI is the overall peak,
SPKI is the running estimate of the signal peak,
NPKI is the running estimate of the noise peak,
THRESHOLD I1 is the first threshold applied, and
THRESHOLD I2 is the second threshold applied.

A peak is a local maximum determined by observing when the signal changes direction within a predefined time interval. The signal peak SPKI is a peak that the algorithm has already established to be a *QRS* complex. The noise peak NPKI is any peak

that is not related to the *QRS* (e.g., the *T* wave). The thresholds are based upon running estimates of SPKI and NPKI. That is, new values of these variables are computed in part from their prior values. When a new peak is detected, it must first be classified as a noise peak or a signal peak. To be a signal peak, the peak must exceed THRESHOLD I1 as the signal is first analyzed or THRESHOLD I2 if searchback is required to find the *QRS*. When the *QRS* complex is found using the second threshold,

$$\text{SPKI} = 0.25\ \text{PEAKI} + 0.75\ \text{SPKI}. \tag{16}$$

The set of thresholds applied to the filtered ECG is determined from

$$\text{SPKF} = 0.125\ \text{PEAKF} + 0.875\ \text{SPKF} \quad \text{(if PEAKF is the signal peak)} \tag{17}$$

$$\text{NPKF} = 0.125\ \text{PEAKF} + 0.875\ \text{NPKF} \quad \text{(if PEAKF is the noise peak)} \tag{18}$$

$$\text{THRESHOLD F1} = \text{NPKF} + 0.25\ (\text{SPKF} - \text{NPKF}) \tag{19}$$

$$\text{THRESHOLD F2} = 0.5\ \text{THRESHOLD F1} \tag{20}$$

where all the variables refer to the filtered ECG:

PEAKF is the overall peak,
SPKF is the running estimate of the signal peak,
NPKF is the running estimate of the noise peak,
THRESHOLD F1 is the first threshold applied, and
THRESHOLD F2 is the second threshold applied.

When the *QRS* complex is found using the second threshold,

$$\text{SPKF} = 0.25\ \text{PEAKF} + 0.75\ \text{SPKF}. \tag{21}$$

For irregular heart rates, the first threshold of each set is reduced by half so as to increase the detection sensitivity and to avoid missing beats:

$$\text{THRESHOLD I1} \leftarrow 0.5\ \text{THRESHOLD I1} \tag{22}$$

$$\text{THRESHOLD F1} \leftarrow 0.5\ \text{THRESHOLD F1}. \tag{23}$$

To be identified as a *QRS* complex, a peak must be recognized as such a complex in both the integration and bandpass-filtered waveforms.

Adjusting the Average RR Interval and Rate Limits

Two *RR*-interval averages are maintained. One is the average of the eight most-recent beats. The other is the average of the eight most-recent beats having *RR* intervals that fall within certain limits. The reason for maintaining these two separate averages is to be able to adapt to quickly changing or irregular heart rates. The first average is the mean of the eight most-recent sequential *RR* intervals regardless of their values.

$$RR\ \text{AVERAGE1} = 0.125\ (RR_{n-7} + RR_{n-6} + \cdots + RR_n) \tag{24}$$

where RR_n is the most-recent *RR* interval.

The second average is based on selected beats.

$$RR\ \text{AVERAGE2} = 0.125\ (RR'_{n-7} + RR'_{n-6} + \cdots + RR'_n) \tag{25}$$

where RR'_n is the most recent *RR* interval that fell between the acceptable low and high *RR*-interval limits. The *RR*-interval limits are

$$RR\ \text{LOW LIMIT} = 92\%\ RR\ \text{AVERAGE2} \tag{26}$$

$$RR\ \text{HIGH LIMIT} = 116\%\ RR\ \text{AVERAGE2}. \tag{27}$$

$$RR\ \text{MISSED LIMIT} = 166\%\ RR\ \text{AVERAGE2} \tag{28}$$

If a *QRS* complex is not found during the interval specified by the *RR* MISSED LIMIT, the maximal peak reserved between the two established thresholds is considered to be a *QRS* candidate.

If each of the eight most-recent sequential *RR* intervals that are calculated from *RR* AVERAGE1 is between the *RR* LOW LIMIT and the *RR* HIGH LIMIT, we interpret the heart rate to be regular for these eight heart beats and

$$RR\ \text{AVERAGE2} \leftarrow RR\ \text{AVERAGE1}. \tag{29}$$

This is the case for normal sinus rhythm.

T-Wave Identification

When an *RR* interval is less than 360 ms (it must be greater than the 200 ms latency), a judgment is made to determine whether the current *QRS* complex has been correctly identified or whether it is really a *T* wave. If the maximal slope that occurs during this waveform is less than half that of the *QRS* waveform that preceded it, it is identified to be a *T* wave; otherwise, it is called a *QRS* complex.

Evaluation

We used the MIT/BIH arrhythmia database to evaluate the *QRS* detection algorithm [8]. The database consists of 48 half-hour recordings for a total of 24 h of ECG data. The database is on four-channel FM magnetic tape. Channels 1 and 2 are the two-channel ECG signals. Channel 3 is an annotation channel recorded in a standard binary format, and channel 4 is a binary-recorded timing track.

Fig. 6 shows the experimental setup for evaluation of the *QRS* algorithm. It includes two four-channel FM tape recorders, two Z80-based laboratory microcomputer systems, a dc amplifier, and a nonfade oscilloscope.

Using the *QRS* detection algorithm, one of the microcomputer systems samples and analyzes the database ECG played back from one of the FM recorders. If it detects a *QRS* complex, it generates a pulse. Simultaneously, the second microcomputer monitors the encoded beat annotation channel of the recorder and generates a pulse coincident with the fiducial mark annotated in the database.

A second four-channel FM tape recorder records the original ECG waveform being analyzed on one channel and the pulses from each of the microcomputer systems on two other channels. All of these signals appear on a nonfade display oscilloscope or a chart recorder for further visual evaluation.

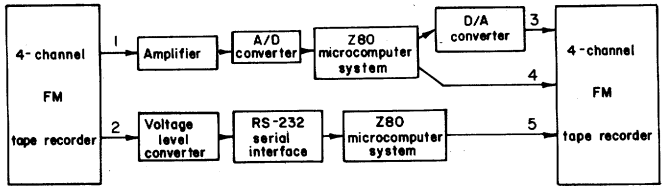

Fig. 6. Experimental setup for evaluating the *QRS* detection algorithm using the MIT/BIH database. *1:* ECG signal from MIT/BIH database channel 1. *2:* Binary annotation from MIT/BIH database channel 3. *3:* Sampled and reconstructed ECG signal. *4:* Pulse generated by detection algorithm. *5:* Pulse obtained from annotation track fiducial mark.

TABLE I
RESULTS OF EVALUATING THE REAL-TIME *QRS* DETECTION ALGORITHM USING THE MIT/BIH DATABASE

Tape (No.)	Total (No. Beats)	FP (Beats)	FN (Beats)	Failed Detection (Beats)	Failed Detection (%)
100	2273	0	0	0	0
101	1865	5	3	8	0.43
102	2187	0	0	0	0
103	2084	0	0	0	0
104	2230	1	0	1	0.04
105	2572	67	22	89	3.46
106	2027	5	2	7	0.05
107	2137	0	2	2	0.09
108	1763	199	22	221	12.54
109	2532	0	1	1	0.04
111	2124	1	0	1	0.05
112	2539	0	1	1	0.04
113	1795	0	0	0	0
114	1879	3	17	20	1.06
115	1953	0	0	0	0
116	2412	3	22	25	1.04
117	1535	1	1	2	0.13
118	2275	1	0	1	0.04
119	1987	1	0	1	0.05
121	1863	4	7	11	0.59
122	2476	1	1	2	0.08
123	1518	0	0	0	0
124	1619	0	0	0	0
200	2601	6	3	9	0.35
201	1963	0	10	10	0.51
202	2136	0	4	4	0.19
203	2982	53	30	83	2.78
205	2656	0	2	2	0.08
207	1862	4	4	8	0.43
208	2956	4	14	18	0.60
209	3004	3	0	3	0.10
210	2647	2	8	10	0.38
212	2748	0	0	0	0
213	3251	1	2	3	0.09
214	2262	2	4	6	0.26
215	3363	0	1	1	0.03
217	2208	4	6	10	0.45
219	2154	0	0	0	0
220	2048	0	0	0	0
221	2427	2	0	0	0.08
222	2484	101	81	182	7.33
223	2605	1	0	1	0.04
228	2053	25	5	30	1.46
230	2256	1	0	1	0.04
231	1886	0	0	0	0
232	1780	6	1	7	0.39
233	3079	0	1	1	0.03
234	2753	0	0	0	0
48 patients	116 137	507	277	784	0.675

The maximal amplitude of the ECG from the FM recorder is less than ±1 V, so a dc amplifier amplifies the signal by a gain of 2.5 to ensure that the signal uses the full range of the A/D converter (the input voltage range is ±2.5 V).

The 24 h MIT/BIH database contains more than 116 000 beats. Table I summarizes the performance of our algorithm for this database. It produced 507 false positive beats (0.437 percent) and 277 false negative beats (0.239 percent) for a total detection failure of 0.675 percent.

The problem tapes are characterized, in general, by stretches of noise, baseline shifts, and artifacts. Tape 108 has unusually tall, peaked *P* waves quite uncharacteristic in morphology of typical *P* waves. Particularly at the beginning and end of this tape, these *P* waves are classified as *QRS* complexes because of their high slopes. This leads to a high false positive count on this tape. Tape 222 also has some non-*QRS* waves with highly unusual morphologies that lead to false positives. A false positive detection for one of these bizarre waveshapes can sometimes lead to a false negative on the following *QRS* complex because the algorithm includes a latency time from the time a *QRS* is detected to the next permitted detection.

SUMMARY

We have developed an on-line real-time *QRS* detection algorithm and implemented it in Z80 assembly language. This algorithm reliably detects *QRS* complexes using slope, amplitude, and width information. A bandpass filter preprocesses the signal to reduce interference, permitting the use of low-amplitude thresholds in order to get high detection sensitivity. In the algorithm, we use a dual-thresholds technique and search-back for missed beats.

The algorithm periodically adapts each threshold and *RR* interval limit automatically. This adaptive approach provides for accurate use on ECG signals having many diverse signal characteristics, *QRS* morphologies, and heart rate changes. In evaluations using the MIT/BIH arrhythmia database, the algorithm failed to properly detect only 0.675 percent of the beats.

REFERENCES

[1] N. V. Thakor, J. G. Webster, and W. J. Tompkins, "Design, implementation, and evaluation of a microcomputer-based portable arrhythmia monitor," *Med. Biol. Eng. Comput.*, vol. 22, pp. 151–159, 1984.

[2] R. G. Mark, G. B. Moody, W. H. Olson, S. K. Peterson, P. S. Schulter, and J. B. Walters, Jr., "Real-time ambulatory arrhythmia analysis with a microcomputer," *Comput. Cardiol.*, pp. 57–62, 1979.

[3] L. Patomaki, J. Forsti, V-M. Nokso-Koivisto, Y. Jokinen, and E. Lansimies, "On line recording and analysis of the ECG in ambulatory patients," *Comput. Cardiol.*, pp. 173–175, 1981.

[4] O. Pahlm and L. Sornmo, "Software QRS detection in ambulatory monitoring–A review," *Med. Biol. Eng. Comput.*, vol. 22, pp. 289–297, 1984.

[5] M. L. Ahlstrom and W. J. Tompkins, "Automated high-speed analysis of Holter tapes with microcomputers," *IEEE Trans. Biomed. Eng.*, vol. BME-30, pp. 651–657, Oct. 1983.

[6] M. Nygards and L. Sornmo, "A QRS delineation algorithm with low sensitivity to noise and morphology changes," *Comput. Cardiol.*, pp. 347–350, 1981.

[7] A. Ligtenberg and M. Kunt, "A robust-digital QRS-detection algorithm for arrhythmia monitoring," *Comput. Biomed. Res.*, vol. 16, pp. 273–286, 1983.

[8] "MIT/BIH arrhythmia database–Tape directory and format specification," Document BMEC TR00, Mass. Inst. Technol., Cambridge, 1980. Database is available from Bioengineering Division KB-26, Beth Israel Hospital, 330 Brookline Avenue, Boston, MA 02215.
[9] "AHA database." Database is available from Emergency Care Research Institute, 5200 Butler Pike, Plymouth Meeting, PA 19462.
[10] H. G. Goovaerts, H. H. Ros, T. J. vanden Akker, and H. Schneider, "A digital QRS detector based on the principle of contour limiting," *IEEE Trans. Biomed. Eng.*, vol. BME-23, p. 154, 1976.
[11] N. V. Thakor, J. G. Webster, and W. J. Tompkins, "Optimal QRS detector," *Med. Biol. Eng. Comput.*, vol. 21, pp. 343–350, 1983.
[12] P. A. Lynn, "Online digital filter for biological signals: Some fast designs for a small computer," *Med. Biol. Eng. Comput.*, vol. 15, pp. 534–540, 1977.

Jiapu Pan received the M.D. degree in 1962 with a specialty in biophysics in medicine from the Shanghai Second Medical College, Shanghai, People's Republic of China.

Since that time, he has been on the Faculty of the Department of Biophysics of the Shanghai Second Medical College. His background includes research in medical applications of lasers, flow cytometry for single cell analysis and sorting, artificial arm control using electromyographic signals, body surface mapping in electrocardiography, and microcomputer-based medical instrumentation. Recently he spent two years in the United States as a visiting scholar. The first of these was at Case Western Reserve University, Cleveland, OH, and the second year was at the University of Wisconsin, Madison, where he completed the work reported here.

Willis J. Tompkins (S'61–M'66–SM'77) received the B.S. and M.S. degrees in electrical engineering from the University of Maine, Orono, in 1963 and 1965, respectively, and the Ph.D. degree in biomedical electronic engineering from the University of Pennsylvania, Philadelphia, in 1973.

From 1965 to 1968 he was an Electrical Engineer at Sanders Associates, Inc., Nashua, NH, where he worked on research and development of data storage systems. He was employed from 1973 to 1974 at the Hospital of the University of Pennsylvania as a Biomedical Engineer. Since 1974 he has been on the Faculty of the University of Wisconsin, Madison, where his teaching specialty is on the topic of computers in medicine, an area in which he has developed two new courses. His research interests include on-line biomedical computing applications. He is co-editor, with J. G. Webster, of the textbook *Design of Microcomputer-Based Medical Instrumentation* (Englewood Cliffs, NJ: Prentice-Hall, 1981) and co-editor, with J. G. Webster, A. M. Cook, and G. C. Vanderheiden, of the textbook *Electronic Devices for Rehabilitation* (New York: Wiley, 1984).

Dr. Tompkins is a member of the IEEE Engineering in Medicine and Biology Society (currently Region IV Administrative Committee Representative and Vice President for Technical Activities), the IEEE Computer Society, the Association for the Advancement of Medical Instrumentation, and the Biomedical Engineering Society. He is a Registered Professional Engineer in the State of Wisconsin.